Hindawi
Shock and Vibration
Volume 2018, Article ID 2129639, 11 pages
https://doi.org/10.1155/2018/2129639

Research Article

Investigation of Energy Mechanism and Acoustic Emission Characteristics of Mudstone with Different Moisture Contents

Jingdong Jiang[1] **and Jie Xu**[2,3]

[1]*Geotechnical Engineering Department, Nanjing Hydraulic Research Institute, Nanjing 210024, China*
[2]*Geotechnical Research Institute, Hohai University, Nanjing 210098, China*
[3]*Key Laboratory of Ministry of Education for Geomechanics and Embankment Engineering, Hohai University, Nanjing 210098, China*

Correspondence should be addressed to Jie Xu; besurexj@163.com

Received 11 April 2018; Revised 2 July 2018; Accepted 8 July 2018; Published 25 July 2018

Academic Editor: Cristina Castejón

Characteristics of energy accumulation, evolution, and dissipation in conventional triaxial compression of mudstones with different moisture contents were explored. Stress-strain relations and acoustic emission (AE) characteristics of the deformation and failure of rock specimens were analyzed. The densities and rates of stored energy, elastic energy, and dissipated energy under different confining pressures were confirmed. The results demonstrated that the growth rate of absorbed total energy decreases with the increase of moisture content, indicating that the higher the moisture content is, the less the total energy mudstone samples absorb. The dissipated energy of the soaking sample, by contrast, has the first increase speed, and natural sample comes second at the beginning. When entering the crack stable development stage, the dry sample has the fastest growing rate of dissipated energy, meaning that dissipated energy used for crack propagation gradually decreases with the increase of moisture content. The AE signals significantly enhance at the initial compression stage and plastic deformation stage with the moisture content decreasing. The AE location events at the failure moment decrease as the moisture content increasing. The time that the maximum AE even rate appears is slightly lagged behind the macroscopic failure time, and the AE even rates increase with the decrease of confining pressure. The above results indicate that the water erosion process on rock reduces the cohesive energy and cohesive force, destroys the micromechanical structure, and minimizes the energy states of rock.

1. Introduction

The radioactive nuclear waste comes mainly from the waste accompanied with the production of atomic weapons and reactor cores at the nuclear plant. An estimated 440 nuclear power plants worldwide are currently generating more than 20 thousand tons of radioactive waste annually. The harm of low- and intermediate-level radioactive nuclear waste is relatively low, and the disposal measures have run to the period that is relatively mature. The high-level radioactive nuclear waste, by contrast, has a long damping period and does more harm [1–4]. Due to the presence of nuclear radiation from high-level nuclear waste, its disposal site must be well sealed and away from the biosphere to prevent nuclear radiation from harming humans and the natural environment [5–11]. It is recommended to store nuclear waste in deep rock masses in the world, as shown in Figure 1.

The excavation, backfilling, and operation of the nuclear waste repository will change the in situ stress field, temperature, and humidity environment in the deep underground. The occurrence of the excavation damage zone in surrounding rock will greatly enhance the permeability of the surrounding rock and greatly reduce the sealing performance. Generally, rocks (such as granite) usually have disadvantages such as unstable geology, less widespread distribution, and difficulty in recovering damage and permeability after disturbance. Compared with granite, mudstone is a good geological material to seal nuclear radiation. Selecting mudstone as the surrounding rock of the repository has four advantages: (1) Mudstone is a sedimentary rock, which is generally found in structurally stable areas around the earth, and the cost of building a reservoir is relatively low. (2) The geochemical properties of mudstone are stable. (3) Mudstone has low permeability and diffusivity, which is

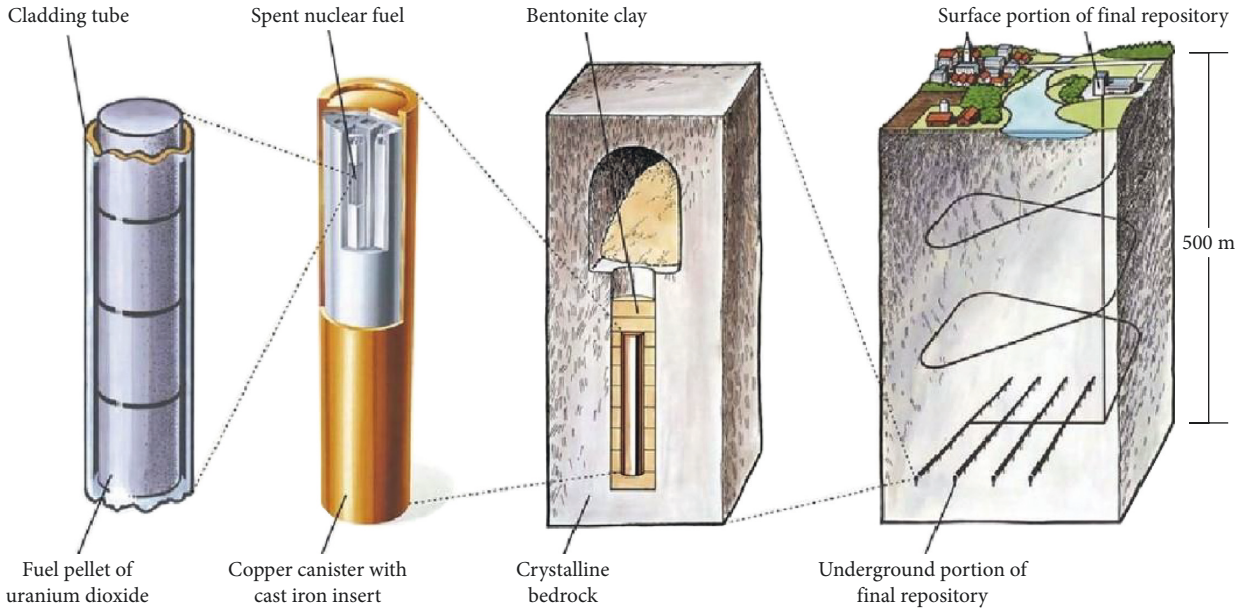

Figure 1: KBS-3 concept of multiple barrier system of SKB in Sweden [12].

not conducive to the penetration and diffusion of radiation particles. (4) Mudstone has strong deformation ability. The damage can be partially restored during long-term operation, and the permeability will be restored significantly with the repair of the damage.

Due to its unique physical and chemical properties, mudstone is extremely sensitive to environmental factors such as temperature, humidity, stress, and groundwater. Especially when the humidity conditions change, the nature and state of the mudstone will change greatly, resulting in hydration expansion and strength reduction, resulting in large deformation or even collapse of the roadway, diverticulum, building matrix, and so on. Therefore, studying the physical and mechanical properties of mudstone under different water-bearing conditions is a subject with theoretical and practical engineering application value [13–17]. He-hua and Bin [18] carried out creep tests of dry and saturated rock to study the law of rock creep affected by moisture content. Bidgoli and Jing [19] used the discrete element method to study the effect of groundwater on rock deformation and strength characteristics. The results show that water has a greater influence on the deformation parameters of rock and less influence on the elastic deformation parameters. Gutierrez et al. [20] carried out the experimental study on the mechanisms of chalk-fluid interaction, especially for the behavior of petroleum chalk reservoirs during water injection. In order to investigate fluid flow and permeability variations, Zhang et al. [21] conducted uniaxial, biaxial, and triaxial tests on large concrete blocks with randomly distributed fractures and rock core samples. The results showed that the permeability around underground openings depended strongly on stress changes and orientations of the natural fractures. Wang et al. [17] proposed a finite element model considering the coupled effects of seepage, damage, and stress field in heterogeneous rock, and a series of numerical simulations of the initiation of hydraulic fractures and their subsequent propagation were carried out.

Acoustic emission technology is a good way to study the process of rock deformation and destruction [22]. To better understand the factors contributing to the dynamic evolution of rock energy, where fracture deformation and extension may be important, monitoring and imaging via acoustic emission may provide important constraint [23–29], examining the effect of a change of loading rate on the evolution of microcracking through acquisition, analysis, and processing the acoustic emission signals. He et al. [30] performed single-face dynamic unloading tests under the true-triaxial condition using the AE monitoring technique and obtained the relationship of frequency-amplitude of AE signals in rock burst stages. The results showed the AE-accumulated energy release rapidly increased from the unloading state of the rock to its failure. In order to detect the symptoms of developing slope instability, Cheon et al. [31] proposed an improved monitoring apparatus and method to evaluate the damage level by means of an AE technique. Zhou et al. [32] carried out different shear tests on irregular artificial sawtooth joints with different asperity heights, and the change laws of AE signals were detected and analyzed. The results could promote the application of the AE techniques to warn the dynamic shear failure of in situ joints.

Most recent research has shown that soft rock is easy to soften, swell, and disintegrate in water, and different water-containing states have an important influence on the mechanical properties and failure mechanism of rock. However, previous studies tend to analyze the deterioration of mechanical properties of rock under saturated or natural conditions and rarely combine energy mechanism to analyze the effect of water content on rock mechanical properties. Therefore, this paper carried out the conventional triaxial compression test of mudstone in dry state, natural state, and saturated state under different confining pressures. According to the energy evolution law and acoustic emission characteristics, the energy

Figure 2: Undisturbed mudstone samples sealed in plastic bags.

mechanism of mudstone under different water contents is analyzed. The research results will be important for analyzing the stability of rock mass in engineering.

2. Experimental Apparatus and Methodology

2.1. Experimental Samples. The mudstone of this paper, which is pure, delicate, grayish black, and brittle, is collected from Huaibei Gubei Coal Mine, located at −575 m to −648 m underground. The undisturbed samples were sealed in plastic bags immediately after being obtained, shown in Figure 2. Mineral analysis was carried out by the D8 Advance X-ray diffractometer. The mineral composition of mudstone was 19.12% kaolinite, 18.88% illite, 16.47% sodium albite, and 45.53% quartz. The mudstone has a natural density of 2.61 g/cm^3 and a particle density of 2.73 g/cm^3. According to the requirements of international regulations, the test piece is processed into a standard cylindrical rock sample with a diameter of 50 mm and a height of 100 mm. The nonparallelism of the test piece ends is not more than 0.02 mm. The end face is perpendicular to the axis, and the maximum deviation does not exceed 0.2°.

In this paper, it is considered that the water content of rock samples is the same. According to the law of water absorption and water loss, the methods of drying and immersing water are adopted to obtain mudstone samples smaller than and larger than the natural water content. The prepared rock samples are divided into three groups. First group is dried. The drying temperature is 105°C and the drying time is 3 hours. The moisture content of the dried rock samples is expected to be 0.80%. Second group adopts soaking samples in natural environment. The immersion time is 3 hours, and the water content of the immersed rock sample is expected to be about 2.03%. The third group maintains the natural state, and the moisture content of the natural mudstone is about 1.56%.

2.2. Experimental Apparatus and Methodology. Uniaxial and triaxial compression tests were carried out on mudstones with different moisture contents on the RMT-301 rock mechanical test system (Figure 3). The confining pressure is 0, 15, and 30 MPa. The test procedure is as follows: the confining pressure is applied to the set value at a loading rate of 0.1 MPa/s, and then the axial loading rate is loaded at 0.001 mm/s until the integrated stress-strain curve is obtained. The acoustic emission device PCI-II was used for

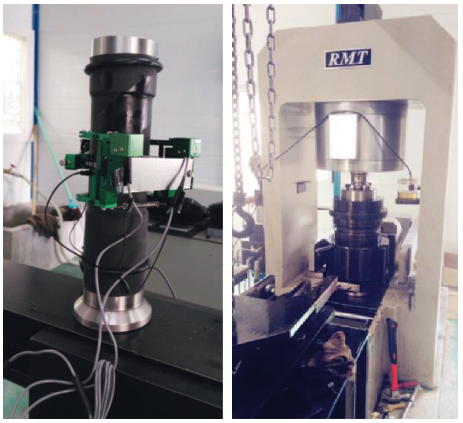

Figure 3: Photographs of the servo-controlled RMT-301.

real-time AE event monitoring during the test, in which the sampling frequency was set to 5 MHz and the threshold was set to 55 dB. In addition, in order to improve the accuracy of three-dimensional positioning of AE events, eight probes are used for data acquisition. Acoustic emissions were monitored with a 16-channel PCI-II system.

3. Energy Mechanism of Mudstone with Different Moisture Contents

3.1. Energy Principle during Rock Failure Process. The exterior loads can result in the deformation in the rock unit. The first law of thermodynamics shows that the deformation of the rock unit is usually regarded as a closed-loop system, and there is no heat exchange between the mechanical work and the environment. The total input energy U is equal to the stored energy of a unit volume rock mass, which is the sum of the releasable elastic strain energy U^{e} and dissipative energy U^{d}. The expression is shown in the following equation:

$$U = U^{\mathrm{e}} + U^{\mathrm{d}}. \tag{1}$$

Under uniaxial compression, the equations of total stored energy and releasable elastic strain energy are expressed as

$$\begin{aligned} U &= \int \sigma_1 \, d\varepsilon_1 = \sum_{i=0}^{n} \frac{1}{2} \left(\varepsilon_{1i+1} - \varepsilon_{1i}\right)\left(\sigma_{1i} + \sigma_{1i+1}\right), \\ U^{\mathrm{e}} &= \frac{\sigma_1^2}{2E_0}, \end{aligned} \tag{2}$$

where σ_{1i} and ε_{1i} are the stress and strain values at every point of the stress-strain curve and E_0 is the elastic modulus.

Under triaxial compression, σ_2 and σ_3 are equal in value, so the equations of total input energy and elastic strain energy read as follows:

$$\begin{aligned} U &= \int \sigma_1 \, d\varepsilon_1 + 2 \int \sigma_3 \, d\varepsilon_3 + U_0, \\ U^{\mathrm{e}} &= \frac{1}{2E_0} \left[\sigma_1^2 + 2\sigma_3^2 - 2\nu\left(2\sigma_1\sigma_3 + \sigma_3^2\right)\right], \end{aligned} \tag{3}$$

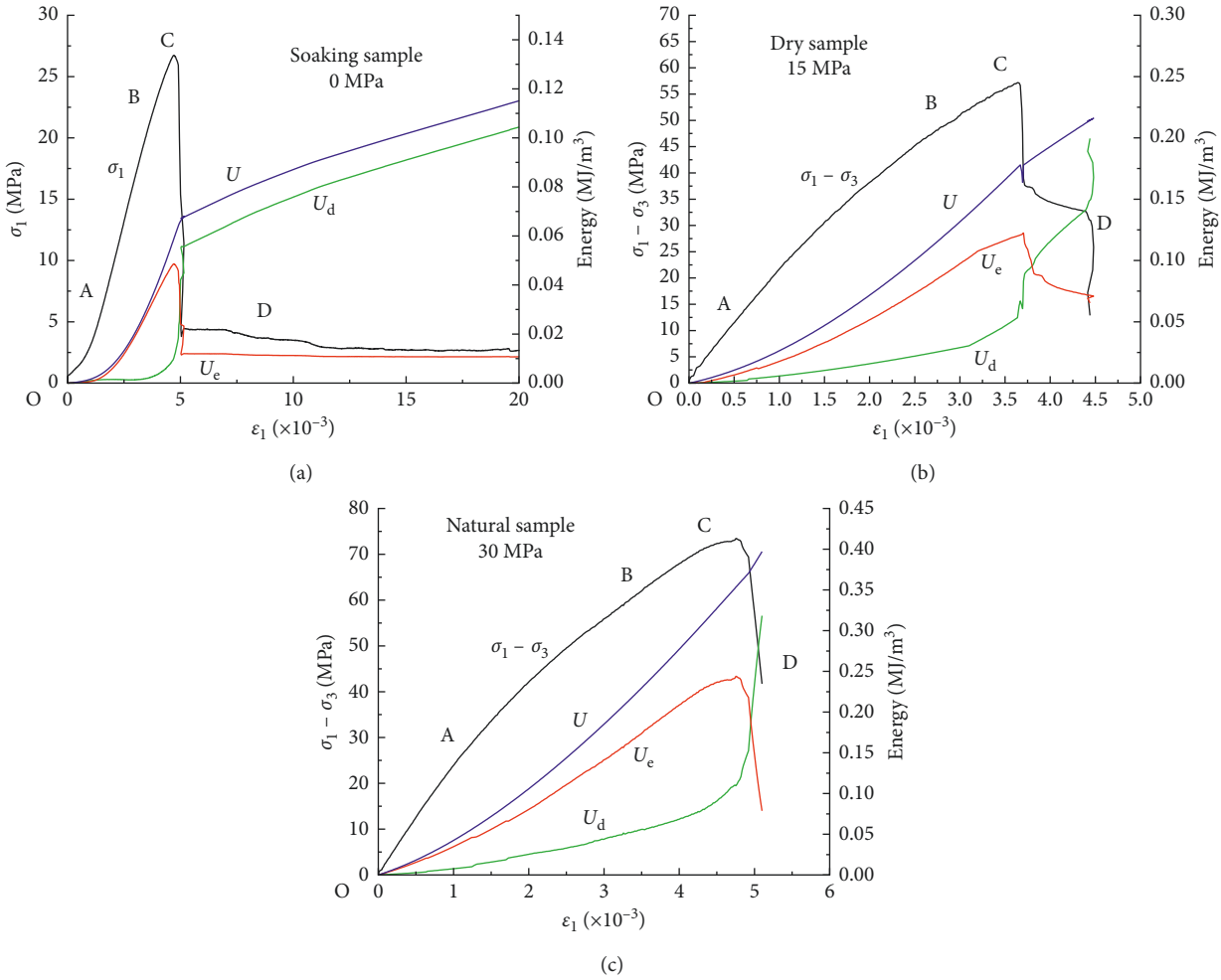

Figure 4: Relation curves of stress and energy with strain for mudstone samples under different moisture contents and confining pressures.

where U_0 is regarded as the strain energy stored under static water pressure in the initial loading, and the equation can be expressed as

$$U_0 = \frac{3(1-2\nu)}{2E_0}(\sigma_3)^2, \tag{4}$$

where E_0 and ν are the initial elastic modulus and Poisson's ratio, respectively.

3.2. Energy Dissipation under the Influence of Moisture Content. According to the thermodynamics, the deformation process of the rock is irreversible, which is accompanied by energy dissipation and energy release. Figure 4 gives the variation of stress and energy of the mudstone samples affected by moisture contents. At the initial compression stage (OA) and line elastic deformation stage (AB), most of the work done by the loads is converted into elastic strain energy stored in the mudstone samples, and a small part turns into dissipated energy. At the stage of the inelastic deformation stage (BC), the growth of elastic strain energy becomes slower with the strain, but the dissipated energy increases gradually. The reason is that the plastic deformation and new cracks begin to gather in the mudstone samples. In addition, the ratio of the dissipated energy to total strain energy has a rapid increase, which could explain that obvious crack propagation and coalescence in rock increases and more damage occurs. When the stress-strain curves enter into the stage of brittle stress drop, the mudstone samples rapidly release the elastic strain energy, and the dissipated energy increases sharply. Almost all of absorbed total energy turns into dissipated energy, which is used for further development of cracks and shear deformation along the slip surface. After failure, the circumferential deformation increases sharply, which results in a rapid increase of negative work done by confining pressure. Therefore, the total energy after failure has a slower growth.

Figure 5 shows the relationship between total energy and strain under different confining pressures. It can be found from the curve that as the water content increases, the total energy absorbed by the mudstone decreases with the increase rate of strain; the higher the water content (saturated sample), the less the total energy absorbed by mudstone, and the lower the water content (dry sample), the more the total energy absorbed by mudstone. This is due to the chemical erosion of water on the rock, which leads to the decrease of the cohesive force of the viscous particles, destroying the internal micromechanical structure and causing the rock to

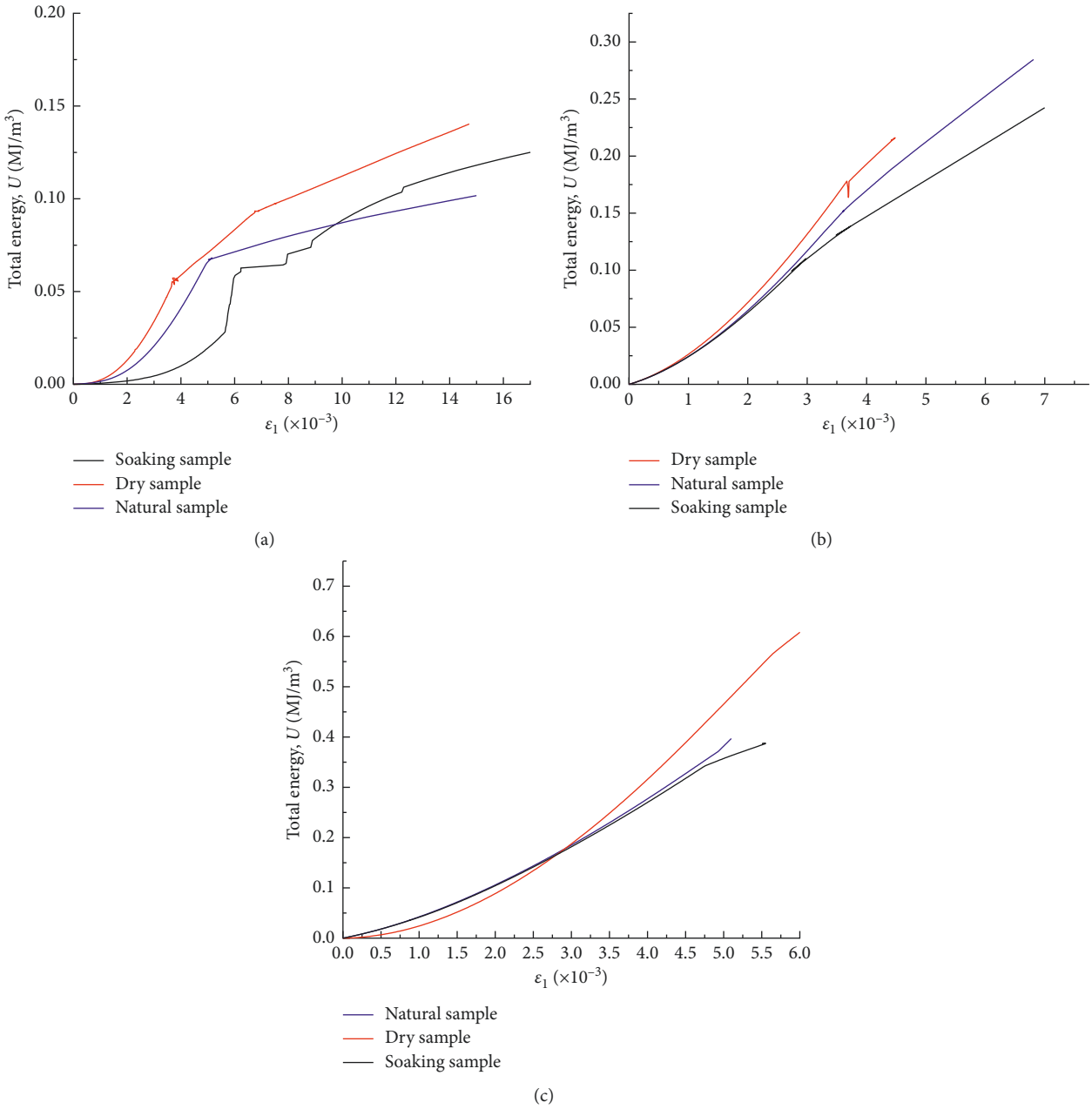

Figure 5: Relation curves of total energy with strain under different confining pressures. (a) 0 MPa. (b) 15 MPa. (c) 30 MPa.

reach a lower energy state. The rock energy storage and energy release are relatively reduced, and the plasticity is enhanced. This is the mechanism that water injection is often used in underground engineering to prevent rock burst.

Figure 6 shows the relationship between dissipation energy and strain under different confining pressures. Dissipated energy is mainly used for the generation and expansion of cracks and the accumulation of damage. It can be seen that, in the compaction phase and the elastic phase, the dissipated energy value is small and the growth is slow. However, the saturated sample grows faster at this stage, and the natural sample grows a little slower. It can be found that the higher the water content is, the more the energy is dissipated. This is mainly due to a series of physical and chemical reactions caused by the interaction of water and rock. So that the water-immersed sample initiates microcrack locally during the loading process, consuming a part of the strain energy. The dry sample is close to the continuous medium after compaction, and the linear elastic characteristic is very obvious. The dissipation energy in the elastic stage is less increased. When entering the elastoplastic stage, the internal cracks of the rock begin to generate and expand, and the proportion of total energy absorbed for dissipation is sharply increased. The growth rate of the dry sample is the fastest, followed by the natural sample, and the saturated sample is relatively lowest. When the rock breaks down, the dissipative energy continues to increase. At this time, the elastic energy accumulated inside the rock is instantaneously

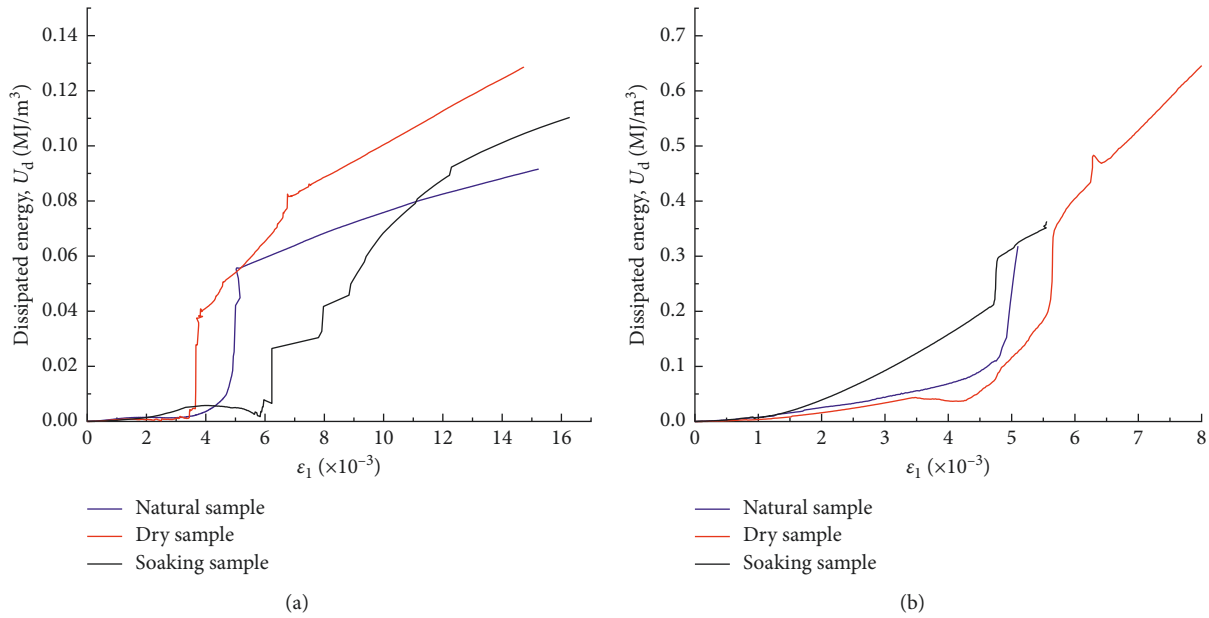

Figure 6: Relation curves of dissipated energy with strain under different confining pressures. (a) 0 MPa. (b) 30 MPa.

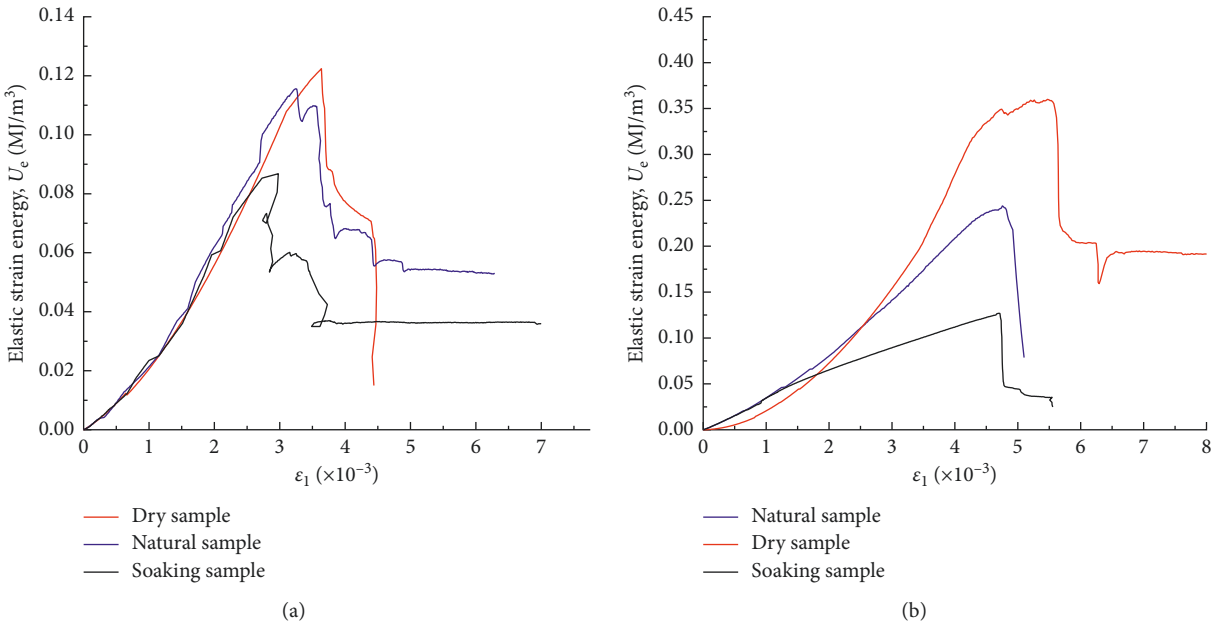

Figure 7: Relation curves of elastic strain energy with strain under different confining pressures. (a) 20 MPa. (b) 30 MPa.

released, and the total energy absorbed by the rock is basically converted into dissipative energy. After the destruction, the dissipative energy of the dry sample still grows fastest, indicating that after entering the elastoplastic stage of stable development of the fracture, the dissipation energy for crack propagation gradually decreases with the increase of water content.

Figure 7 shows the relationship between elastic energy and strain under different confining pressures. In the compaction phase and the elastic phase, the elastic energy stored in the rock increases rapidly, and the total energy absorbed by the rock is basically converted into elastic energy for storage. The storage rates of elastic energy of mudstones in different water-bearing states are quite different, and the lower the water content, the greater the elastic energy during energy storage. After entering the elastoplastic stage, the rate of increase of elastic energy slows down due to the gradual cracking inside the rock. After instability and destruction, the elastic release is a source of power for rock damage. From the stage of stable development of rupture, the lower the water content, the higher the elastic energy stored in the rock. The release rate of the elastic strain energy of the saturated sample is greater than the release rate of the dry sample.

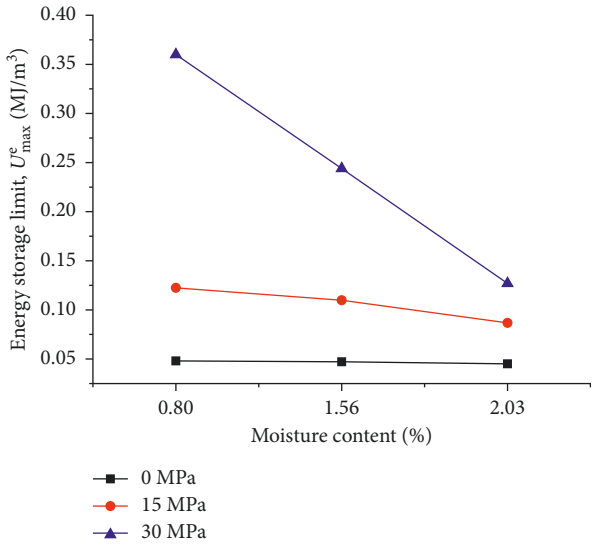

Figure 8: Relationship between energy storage limit and moisture content.

The elastic energy stored inside the rock always has a maximum value from the generation, accumulation to release process, which is usually called the energy storage limit. Figure 8 shows the relationship between energy storage limit and water content under different confining pressure conditions. It can be seen that under the same confining pressure condition, the energy storage limit decreases linearly with the increase of water content; that is, the lower the water content is, the higher the maximum elastic strain energy the rock can store. This is consistent with the analysis results of the previous energy components. In addition, the higher the confining pressure, the greater the ultimate energy storage, indicating that the increase in confining pressure enhances the energy storage capacity of the rock.

4. Acoustic Emission Characteristics of Mudstone Samples with Different Moisture Contents

AE signal can directly reflect the damage accumulation and crack propagation process in rock under the exterior loads. The AE event, cumulative AE events, and AE event rate are the most common AE parameters, and they can form independent time series. The AE event rate can describe the amount of energy released during rock failure, which means the number of AE events per unit of time. The higher AE event rate usually reflects the more severe internal damage of rock. Figure 9 shows the change process of AE event rate for mudstone samples affected by moisture contents. As shown in Figure 9, the AE event rates of complete stress-strain curve of rock at each stage have different characteristics. At the initial loading stage, the AE event rates of mudstone samples with different moisture contents are relatively low, especially soaked samples. The small number of AE events results from the closure of original cracks and porosity, and hardly any new crack generates. When entering into the stage of elastic deformation, the stress-strain curves of mudstone samples are almost linear, so the stiffness of mudstone samples should be nearly constant during loading process. Compared with the initial stage, the AE event rates of mudstone samples at this stage show an increase but still low. When the stress-strain curves step into plastic deformation stage, the AE event rates have a remarkable rise which have increased almost three to five times in the intensity. The results reveal that new cracks begin to emerge and the damage gradually accumulates. With the increase in load, a sudden enhancement of AE signals is found immediately prior to failure, and the cause might be the emergence of a large or persistent crack inside the samples. When entering into the failure stage, there is a step change step in the AE event rate which corresponds to the irregular inflection points in stress-strain curves. At the same time, the spalling and cracks have come out on the rock surfaces. In conclusion, the AE event rates have a significant increase at initial compression stage and plastic deformation stage when the moisture content decreases; the AE signals are more dispersed, and the AE event rates decrease with the moisture content increasing when entering into the failure stage. The above results indicate that the increase of moisture content reduces the brittleness failure characteristics of the mudstone samples.

Nowadays, the AE location method is commonly used in the material crack damage orientation and the investigation of failure process. The failure picture and the corresponding AE location events of the samples are shown in Figure 10. It is found that the AE location events at failure decrease when the moisture content increases. In addition, the failure modes of mudstone samples are closely related to the moisture contents. Specifically, the single shear damage is more likely to emerge with the moisture content decreasing. It can be seen in the failure pictures that only one main control shearing surface runs through the whole sample, dividing the sample into two triangle cone shaped rocks. In contrast, the combination failure mode of single shear and splitting failure is more likely to emerge with the moisture content increasing. When more water molecules enter the gaps of particles, the cementation action is weakened, and the amount of energy required to fracture the particles decreases. That is why the moisture content can influence the failure mode of samples.

Figure 11 shows the variation curve of the acoustic emission event rate of dry samples under different confining pressures. Acoustic emission signals are concentrated in the stage of unstable damage and the stage of destruction development. The high acoustic emission event rate indicates that the rock sample has brittle damage. The maximum time of the acoustic emission event rate appears slightly later than the time when the macroscopic failure of the rock sample occurs. Comparing the acoustic emission activities of mudstones under three confining pressures, it can be found that the acoustic emission event rate generally decreases with the increase of confining pressure. It shows that the smaller the confining pressure, the more severe the internal damage of the rock (Figure 12).

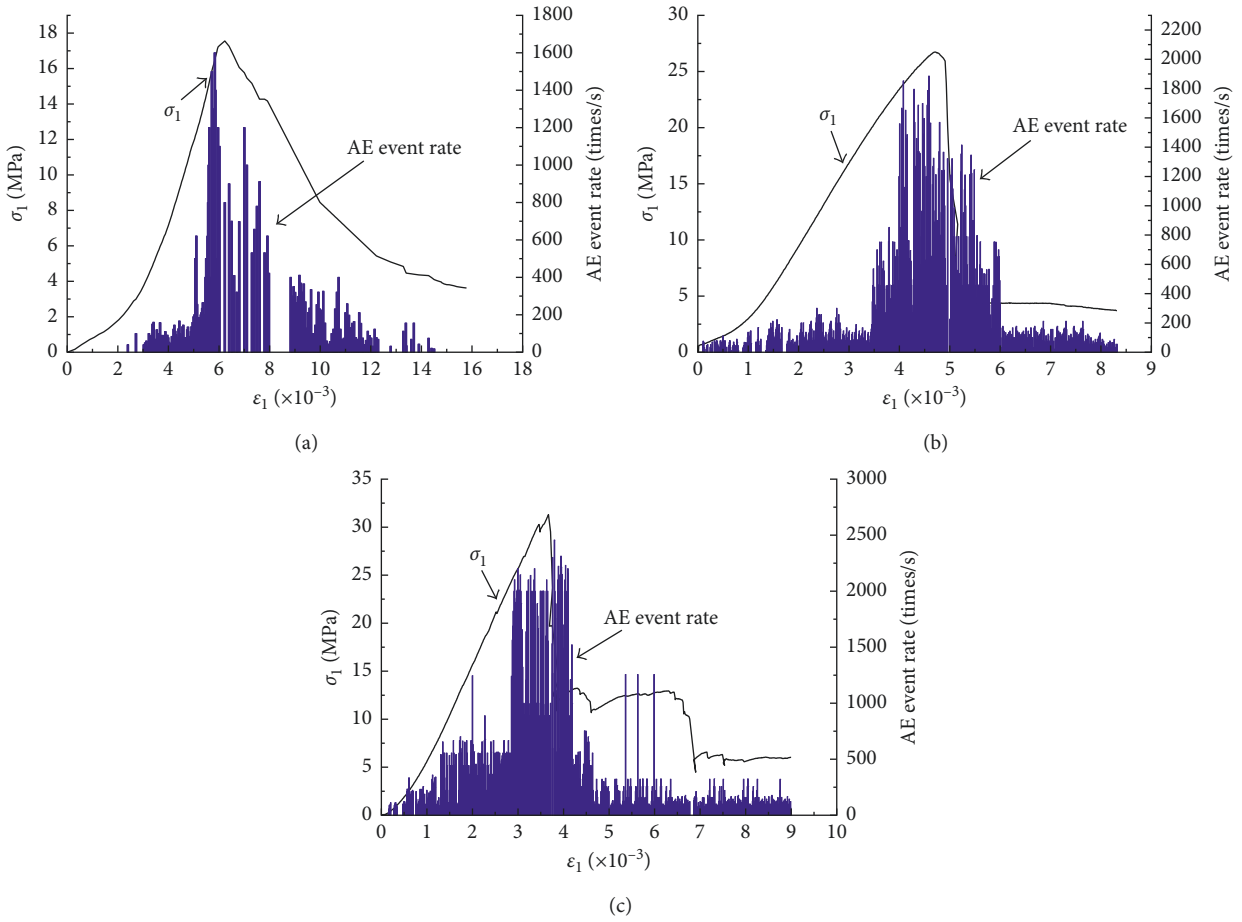

Figure 9: Variation curves of AE event rates for mudstone samples with different moisture content under uniaxial compression. (a) Soaked sample. (b) Natural sample. (c) Dry sample.

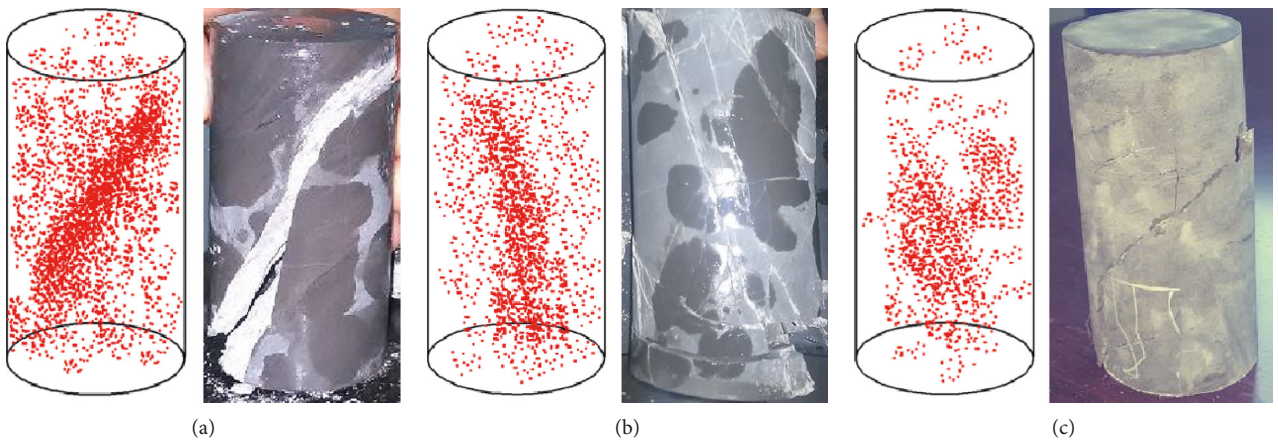

Figure 10: AE location results and failure pictures of mudstone samples with different moisture contents at the moment of rock failure under confining pressure of 15 MPa. (a) Dry sample. (b) Natural sample. (c) Soaked sample.

In the water-immersed state, the structure of the mudstone is destroyed due to the dissolution of the muddy cement and the water swelling of the clay mineral. When moisture content is decreased, the fine particles are attached to the large particles. Then the fluidity between the particles is deteriorated, and the structure is enhanced. Therefore, the strength of the dry sample is increased, and the strength of the saturated sample is lowered. From the energy point of view, the strain energy of the saturated mudstone is higher than that of the dry mudstone during the loading process,

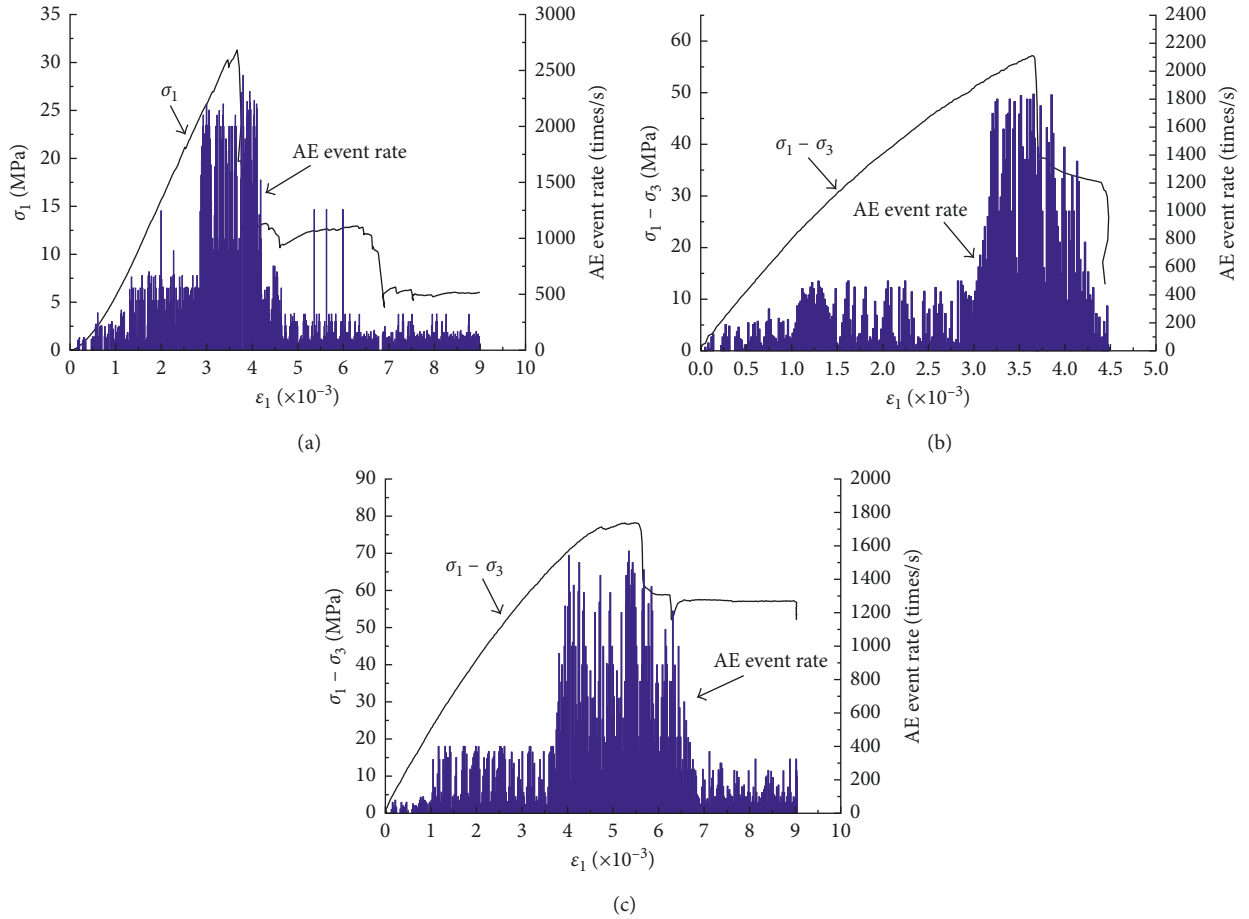

Figure 11: Variation curves of AE event rates for dry samples under different confining pressures. (a) 0 MPa. (b) 15 MPa. (c) 30 MPa.

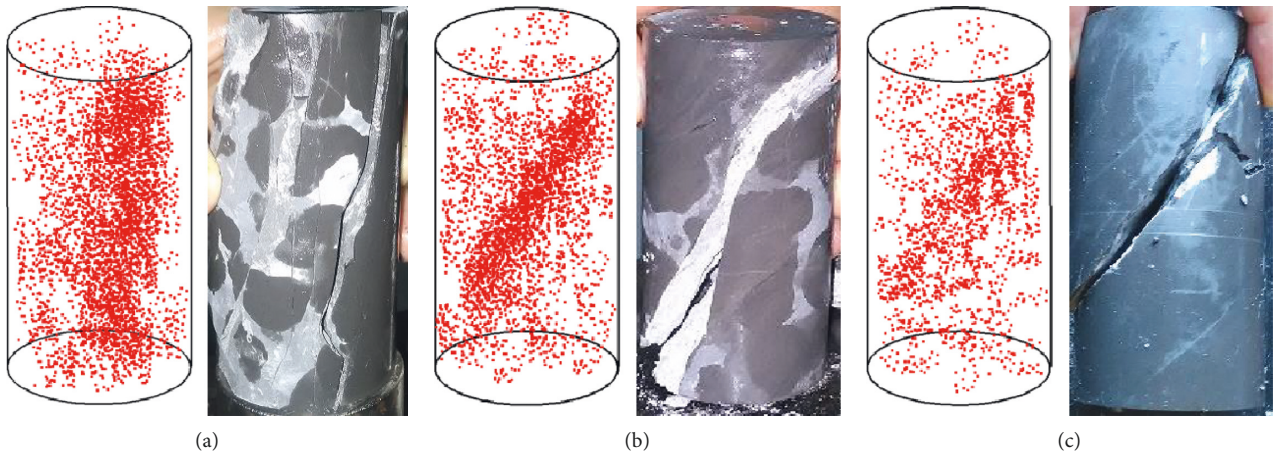

Figure 12: AE location results and failure pictures of dry samples at the moment of rock failure under different confining pressures. (a) 0 MPa. (b) 15 MPa. (c) 30 MPa.

and the energy storage is reduced. At the same time, acoustic emission energy shows that the elastic strain energy released by the saturated sample is lower compared with that by the dried sample at failure. More transformed into plastic deformation energy, indicating that the plasticity of the mudstone increases with the increase of water content. The absorbed energy is more converted into plastic deformation energy. It shows that the plasticity of mudstone increases with the increase of water content. Through research, it is found that water has a great influence on the mechanical properties of mudstone, and the degree of influence is affected by the water content. Therefore, the moisture content

of mudstone must be taken into consideration before the nuclear waste disposal repository is built.

5. Conclusions

The geological disposal in deep underground engineering is a high-level radioactive waste disposal method adopted extensively in the world. The basic principle of this method is to excavate a single- or multitunnel system situated 500–1000 m below the earth's surface and then to place the final form of radioactive waste into preset position and backfill the tunnel system. Compared with other mother rocks, such as granite, rock salt, and shale, mudstone is usually the optimal option. However, the influence of underground water on mudstone is considerable to the stability of high-level radioactive waste disposal repository, but there are few researches on this topic. Based on conventional triaxial compression expression experiments of mudstone specimens with different moisture contents, the following main points are concluded.

The process from rock deformation, failure to collapse, is an irreversible process of energy dissipation, and moisture content has an important impact on this process. In the dry, natural, and saturated states, the total energy absorbed by the mudstone gradually decreases with the increase of the strain. The higher the water content, the less the total energy absorbed by the mudstone. The reason is that water molecules can easily enter clay minerals such as illite and kaolinite, which will weaken the cohesive force among the particles. The dissolution of argillaceous cement and the water swelling of clay minerals will destroy the structure of the mudstone and soften the rock.

The dissipative energy is small and slow in the compaction phase and the elastic phase. The greater the water content is, the more the energy dissipated is. After entering the elastoplastic phase, the total energy absorbed is used to increase the proportion of dissipative effect. The smaller the moisture content, the faster the growth. After the destruction, the dissipative energy of the dry sample still grows faster, indicating that after entering the elastoplastic stage of stable development of the fracture, the dissipation energy for crack propagation gradually decreases with the increase of water content.

The elastic energy storage rate decreases with the increase of moisture content in the compaction stage and the elastic stage. The elastic energy growth rate slows down in the elastoplastic stage. The lower the water content in the instability stage, the higher the storage elastic energy. At the same confining pressure condition, the energy storage limit of mudstone decreases linearly with increasing water content.

The time that the maximum AE even rate appears is slightly lagged behind the macroscopic failure time. The maximum AE event rates during the failure process under uniaxial compression lies in the range of 2200–2500, while those under the confining pressure of 15 MPa and 30 MPa, respectively, fall in the range of 1800–2000 and 1500–1700, indicating that the acoustic emission event rate decreases with the increase of water content and decreases with the increase of confining pressure. The lower the water content and the smaller the confining pressure, the more the internal damage of mudstone.

Data Availability

No data were used to support this study.

Conflicts of Interest

The authors declare that they have no conflicts of interest.

Acknowledgments

This work was supported by the China Postdoctoral Science Foundation (Grant nos. 2017M621782 and 2017M611676), the Jiangsu Province Postdoctoral Research Funding Scheme (Grant nos. 1701026B and 1701091B), and the Basic Scientific Research Project of Central Government-Level Public Welfare Scientific Research Institute (Y317003).

References

[1] H. J. Choi, J. Y. Lee, and J. Choi, "Development of geological disposal systems for spent fuels and high-level radioactive wastes in Korea," *Nuclear Engineering and Technology*, vol. 45, no. 1, pp. 29–40, 2013.

[2] R. P. Rechard, "Milestones for selection characterization and analysis of the performance of a repository for spent nuclear fuel and high-level radioactive waste at Yucca mountain," *Lecture Notes in Control and Information Sciences*, vol. 6, no. 2, pp. 147–157, 2015.

[3] A. Salama, M. F. E. Amin, and S. Sun, "Numerical investigation of high level nuclear waste disposal in deep anisotropic geologic repositories," *Progress in Nuclear Energy*, vol. 85, pp. 747–755, 2015.

[4] B. Johnson, A. Newman, and J. King, "Optimizing high-level nuclear waste disposal within a deep geologic repository," *Annals of Operations Research*, vol. 253, no. 2, pp. 733–755, 2016.

[5] R. C. Ewing and W. J. Weber Jr., "Radiation effects in nuclear waste forms for high-level radioactive waste," *Progress in Nuclear Energy*, vol. 29, no. 2, pp. 63–127, 1995.

[6] E. Sheet, *Final Environmental Impact Statement for a Geologic Repository for the Disposal of Spent Nuclear Fuel and High-Level Radioactive Waste at Yucca Mountain, Nye County, Nevada*, 2002.

[7] A. Millard, A. Rejeb, M. Chijimatsu et al., "Numerical study of the THM effects on the near-field safety of a hypothetical nuclear waste repository-BMT1 of the DECOVALEX III project. Part 2: effects of THM coupling in continuous and homogeneous rocks," *International Journal of Rock Mechanics and Mining Sciences*, vol. 42, no. 5-6, pp. 731–744, 2005.

[8] P. N. Swift, "15-Safety assessment for deep geological disposal of high-level radioactive waste in geological repository systems," in *Geological Repository Systems for Safe Disposal of Spent Nuclear Fuels and Radioactive Waste*, Elsevier, New York, NY, USA, pp. 497–521, 2010.

[9] M. Galamboš and O. Rosskopfová, "Utilization of Slovak bentonites in deposition of high-level radioactive waste and spent nuclear fuel," *Journal of Radioanalytical and Nuclear Chemistry*, vol. 288, no. 3, pp. 765–777, 2011.

[10] A. Dutt, M. S. Saini, T. N. Singh et al., "Analysis of thermo-hydrologic-mechanical impact of repository for high-level radioactive waste in clay host formation: an Indian reference disposal system," *Environmental Earth Sciences*, vol. 66, no. 8, pp. 2327–2341, 2012.

[11] R. P. Rechard, H. H. Liu, Y. W. Tsang, and S. Finsterle, "Site characterization of the Yucca Mountain disposal system for spent nuclear fuel and high-level radioactive waste," *Reliability Engineering and System Safety*, vol. 122, no. 122, pp. 32–52, 2014.

[12] SKB, "Sea disposal of radioactive wastes," Technical Report TR-01-30, IAEA, Vienna, Austria, 2001.

[13] A. Odedra, M. Ohnaka, H. Mochizuki, and P. Sammonds, "Temperature and pore pressure effects on the shear strength of granite in the brittle-plastic transition regime," *Geophysical Research Letters*, vol. 28, no. 15, pp. 3011–3014, 2001.

[14] J. Rutqvist and O. Stephansson, "The role of hydromechanical coupling in fractured rock engineering," *Hydrogeology Journal*, vol. 11, no. 1, pp. 7–40, 2003.

[15] C. A. Tang, T. Xu, T. H. Yang, and Z. Z. Liang, "Numerical investigation of the mechanical behavior of rock under confining pressure and pore pressure," *International Journal of Rock Mechanics and Mining Sciences*, vol. 41, pp. 336–341, 2004.

[16] M. Talesnick and S. Shehadeh, "The effect of water content on the mechanical response of a high-porosity chalk," *International Journal of Rock Mechanics and Mining Sciences*, vol. 44, no. 4, pp. 584–600, 2007.

[17] S. Y. Wang, S. W. Sloan, S. G. Fityus, D. V. Griffiths, and C. A. Tang, "Numerical modeling of pore pressure influence on fracture evolution in brittle heterogeneous rocks," *Rock Mechanics and Rock Engineering*, vol. 46, no. 5, pp. 1165–1182, 2013.

[18] Z. He-hua and Y. Bin, "Experimental study on mechanical properties of rock creep in saturation," *Chinese Journal of Rock Mechanics and Engineering*, vol. 21, no. 12, pp. 1791–1796, 2002.

[19] M. N. Bidgoli and L. Jing, "Water pressure effects on strength and deformability of fractured rocks under low confining pressures," *Rock Mechanics and Rock Engineering*, vol. 48, no. 3, pp. 971–985, 2015.

[20] M. Gutierrez, L. E. Oino, and K. Hoeg, "The effect of fluid content on the mechanical behavior of fractures in chalk," *Rock Mechanics and Rock Engineering*, vol. 33, no. 2, pp. 93–117, 2000.

[21] J. Zhang, W. B. Standifird, J. C. Roegiers, and Y. Zhang, "Stress-dependent fluid flow and permeability in fractured media: from lab experiments to engineering application," *Rock Mechanics and Rock Engineering*, vol. 40, no. 1, pp. 3–21, 2007.

[22] D. Lockner, "The role of acoustic emission in the study of rock fracture," *International Journal of Rock Mechanics and Mining Sciences and Geomechanics Abstracts*, vol. 30, no. 7, pp. 883–899, 1993.

[23] I. Yamada, K. Masuda, and H. Mizutani, "Electromagnetic and acoustic emission associated with rock fracture," *Physics of the Earth and Planetary Interiors*, vol. 57, no. 1, pp. 157–168, 1989.

[24] E. Eberhardt, D. Stead, B. Stimpson, and R. S. Read, "Identifying crack initiation and propagation thresholds in brittle rock," *Canadian Geotechnical Journal*, vol. 35, no. 2, pp. 222–233, 1998.

[25] M. Cai, P. K. Kaiser, H. Morioka et al., "FLAC/PFC coupled numerical simulation of AE in large-scale underground excavations," *International Journal of Rock Mechanics and Mining Sciences*, vol. 44, no. 4, pp. 550–564, 2007.

[26] S. H. Chang and C. I. Lee, "Estimation of cracking and damage mechanisms in rock under triaxial compression by moment tensor analysis of acoustic emission," *International Journal of Rock Mechanics and Mining Sciences*, vol. 41, no. 7, pp. 1069–1086, 2004.

[27] H. Wang and M. Ge, "Acoustic emission/microseismic source location analysis for a limestone mine exhibiting high horizontal stresses," *International Journal of Rock Mechanics and Mining Sciences*, vol. 45, no. 5, pp. 720–728, 2008.

[28] Z. A. Moradian, G. Ballivy, and P. Rivard, "Application of acoustic emission for monitoring shear behavior of bonded concrete-rock joints under direct shear test," *Canadian Journal of Civil Engineering*, vol. 39, no. 8, pp. 887–896, 2012.

[29] T. Backers, S. Stanchits, and G. Dresen, "Tensile fracture propagation and acoustic emission activity in sandstone: the effect of loading rate," *International Journal of Rock Mechanics and Mining Sciences*, vol. 42, no. 7, pp. 1094–1101, 2005.

[30] M. C. He, J. L. Miao, and J. L. Feng, "Rock burst process of limestone and its acoustic emission characteristics under true-triaxial unloading conditions," *International Journal of Rock Mechanics and Mining Sciences*, vol. 47, no. 2, pp. 286–298, 2010.

[31] D. S. Cheon, Y. B. Jung, E. S. Park, W. K. Song, and H. I. Jang, "Evaluation of damage level for rock slopes using acoustic emission techniques with waveguides," *Engineering Geology*, vol. 121, no. 1, pp. 75–88, 2011.

[32] H. Zhou, F. Z. Meng, C. Q. Zhang, D. W. Hu, J. J. Lu, and R. C. Xu, "Investigation of the acoustic emission characteristics of artificial saw-tooth joints under shearing condition," *Acta Geotechnica*, vol. 11, no. 4, pp. 925–939, 2014.